Bridging oxygen as a site for proton adsorption on the vitreous silica surface

Glenn K. Lockwood and Stephen H. Garofalini[a)]
Department of Materials Science and Engineering, Interfacial Molecular Science Laboratory, Rutgers University, Piscataway, New Jersey 08855, USA

(Received 10 June 2009; accepted 25 July 2009; published online 18 August 2009)

Molecular dynamics computer simulations were used to study the protonation of bridging oxygen (Si–O–Si) sites present on the vitreous silica surface in contact with water using a dissociative water potential. In contrast to first-principles calculations based on unconstrained molecular analogs, such as $H_7Si_2O_7^+$ molecules, the very limited flexibility of neighboring SiO_4 tetrahedra when embedded in a solid surface means that there is a relatively minor geometric response to proton adsorption, requiring sites predisposed to adsorption. Simulation results indicate that protonation of bridging oxygen occurs at predisposed sites with bridging angles in the 125°–135° range, well below the bulk silica mean of ~150°, consistent with various *ab initio* calculations, and that a small fraction of such sites are present in all ring sizes. The energy differences between dry and protonated bridges at various angles observed in the simulations coincide completely with quantum calculations over the entire range of bridging angles encountered in the vitreous silica surface. Those sites with bridging angles near 130° support adsorbed protons more stably, resulting in the proton remaining adsorbed for longer periods of time. Vitreous silica has the necessary distribution of angular strain over all ring sizes to allow protons to adsorb onto bridging oxygen at the surface, forming acidic surface groups that serve as ideal intermediate steps in proton transfer near the surface. In addition to hydronium formation and water-assisted proton transfer in the liquid, protons can rapidly move across the water-silica interface via strained bridges that are predisposed to transient proton adsorption. Thus, an excess proton at any given location on a silica surface can move by either water-assisted or strained bridge-assisted diffusion depending on the local environment. The result of this would be net migration that is faster than it would be if only one mechanism is possible. These simulation results indicate the importance of performing large size and time scale simulations of the structurally heterogeneous vitreous silica exposed to water to describe proton transport at the interface between water and the silica surface. © *2009 American Institute of Physics*.
[DOI: 10.1063/1.3205946]

I. INTRODUCTION

Understanding the nature of hydrated silica surfaces has been an area of a great amount of interest for many decades,[1–23] with applications in optical communications,[24] microelectronic and micromechanical devices,[25] geosciences,[26–28] and nuclear technology.[29] In these materials, surface chemistry plays an important role in the overall material properties, and the state of hydration governs the ability for such materials to be used or functionalized for various applications. For instance, recent work has shown increased proton conduction in nanoporous silica as a function of water content.[30–32] The mechanism is believed to be related to the formation of hydronium ions near the silica surface and proton transport between these species and water or along the silica surface, but details are experimentally elusive. Computational techniques offer a complementary approach to address water-silica behavior.

Molecular orbital calculations have been used to simulate molecules which serve as discrete analogs to specific surface sites, and many of these studies have described potential sites for water adsorption or reaction on silica surfaces.[26,33–36] More recently, this first-principles approach has been extended via *ab initio* molecular dynamics (MD) to reveal more complex interfacial phenomena such as the role of molecular water in proton transport after a reaction[23,37] and the formation of different chemisorbed hydroxyl species at different surface sites.[38]

Classical MD simulations have also been used to probe the formation of hydrated species at the silica surface.[9,15,39] While some have implemented dissociative interatomic potentials,[40,41] the majority of MD simulations performed on water-silica interfaces have used nondissociative water models to describe the liquid phase and have involved manually placing protons at specific silica surface sites to emulate existing models of the hydrated surface (e.g., Refs. 12, 42, and 43). Thus, the only surface species present in these latter simulations are those that are prescribed at the beginning, and the majority of water-silica studies, both experimental and computational, regard SiOH as the only surface group of interest.

However, recent experimental studies have indicated the presence of $SiOH_2^+$ on the surface in addition to SiOH,[44] and

[a)]Electronic mail: shg@rutgers.edu.

this $SiOH_2^+$ group has been observed in MD simulations of water reactions on silica[15] that have applied the same the dissociative water potential used in this work. In addition, several studies based in first-principles calculations have concerned themselves with the effect of hydrogen on a siloxane bridge in the context of mineral dissolution. Early molecular orbital calculations showed that when an excess proton adsorbs on a Si–O–Si bridge, the bridging angle narrows and the Si–O bonds weaken.[35] A later study using a more detailed quantum description established that the formation of these bridging OH (BOH) species is thermodynamically favored in the context of H_3O^+-catalyzed dissolution of silicates,[45] although subsequent *ab initio* calculations that incorporated the effects of hydronium solvation in a single solvation shell of water have suggested that the formation of these protonated bridges is energetically unfavorable, and appreciable concentrations should not exist outside of highly acidic systems.[46] However, proton transport via the H_3O^+ ion has been shown to depend significantly on the interaction of the hydronium's first neighbor waters in the Eigen complex with the second neighbor waters,[47] enabling closer interaction between the hydronium ion and one water in a Zundel complex. Thus, while accounting for the first water neighbors was an improvement in accuracy in the aforementioned work by Criscenti *et al.*, accounting for those additional water molecules that surround the H_3O^+ ion's first neighbor waters could significantly modify the activation barrier to transfer.

Additional *ab initio* studies motivated by the experimental observation of mobile protons in silica[48] have indicated that protons can associate with bridges in the silica network,[49] and a higher degree of strain in the glass results in protons which can move between bridges more easily.[50] These quantum mechanical studies performed on molecules and small clusters provide a foundation for the existence of protonated bridging oxygens (BOs) at the interface between silica and water. Thus, certain bridges at the silica-water interface should serve as adsorption sites for excess protons, and these sites may contribute to the anomalously high proton conductivity observed in wet nanoporous silica glasses.[30] Because of the complexity of the interactions at the silica surface with a sufficient number of water molecules nearby, the role of longer range siloxane connectivity neglected in the previously mentioned *ab initio* calculations, and the structural heterogeneity of the silica surface, simulations of larger length and time scales are necessary for a more accurate understanding of the behavior of protons at BOs on silica.

In this study, MD simulations were performed to characterize the formation of such BOH sites on vitreous silica surfaces using a dissociate water interatomic potential that matches many of the properties of bulk water.[41] Application of this dissociative potential to silica-water reactions has shown results consistent with both experiment and *ab initio* calculations.[15] Specifically, $\sim$4.2 $SiOH/nm^2$ form on the silica surface, including the presence of $SiOH_2^+$, and an enhanced formation of H_3O^+ ions occurs. The mechanism and time evolution of the transfer of the H^+ ion via adjacent water molecules occur in the same manner as seen in *ab initio* MD simulations.[15,37] Simulating the water-silica interface using classical MD and an accurate dissociative potential function for water has enabled a much more comprehensive analysis to be made due to the larger system size and time scale possible. A quantitative description of the energetics and geometry of this proton adsorption site over large vitreous silica surfaces, consistent with quantum results, is presented.

II. COMPUTATIONAL PROCEDURE

A. Interatomic potential

MD simulations were carried out by integrating classical equations of motion using a fifth-order Nordsieck–Gear algorithm using a fully atomistic multibody potential to describe the interactions between atoms. These interactions were described using a dissociative water potential developed previously,[41] which is comprised of two- and three-body terms. The two-body contribution consists of point-charge (q) and diffuse-charge (qd) Coulomb interactions and short-range repulsive and dispersive interactions, given by

$$U_{ij}^{\text{2-body}}(r_{ij}) = U_{ij}^{q-q} + U_{ij}^{qd-qd} + U_{ij}^{q-qd} + U_{ij}^{qd-q} + U_{ij}^{\text{rep}} + U_{ij}^{\text{disp}}, \tag{1}$$

where each energy term is a function of the interatomic spacing r_{ij} and is given by

$$U_{ij}^{q-q}(r_{ij}) = \frac{q_i q_j}{r_{ij}} \text{erfc}\left(\frac{r_{ij}}{\beta}\right), \tag{2}$$

$$U_{ij}^{qd-qd}(r_{ij}) = \frac{q_i^d q_j^d}{r_{ij}} \text{erf}\left(\frac{r_{ij}}{2\xi_{ij}}\right) \text{erfc}\left(\frac{r_{ij}}{\beta}\right), \tag{3}$$

$$U_{ij}^{q-qd}(r_{ij}) = \frac{q_i q_j^d}{r_{ij}} \text{erf}\left(\frac{r_{ij}}{\sqrt{2}\xi_{ij}}\right) \text{erfc}\left(\frac{r_{ij}}{\beta}\right), \tag{4}$$

$$U_{ij}^{qd-q}(r_{ij}) = \frac{q_i^d q_j}{r_{ij}} \text{erf}\left(\frac{r_{ij}}{\sqrt{2}\xi_{ij}}\right) \text{erfc}\left(\frac{r_{ij}}{\beta}\right), \tag{5}$$

$$U_{ij}^{\text{rep}}(r_{ij}) = A_{ij}^{\text{rep}} \frac{2\xi_{ij}^r}{r_{ij}} \text{erfc}\left(\frac{r_{ij}}{2\xi_{ij}^r}\right), \tag{6}$$

$$U_{ij}^{\text{disp}}(r_{ij}) = -\frac{C_{ij}^6}{r_{ij}^6}. \tag{7}$$

The parameters used in this study are listed in Table I. ξ_{OH}^r is calculated as a function of temperature and pressure as described elsewhere.[41] The calculated interactions between pairs are limited to atoms separated by a distance less than $R_c = 10$ Å. The long-range Coulomb interactions are corrected by using the Wolf summation method,[51] which has been applied in past work and the details of its application can be found elsewhere.[41,51] The point charges q and diffuse charges q^d assigned to each type of atom are listed in Table II.

The three-body portion of the interatomic potential is a function of the interatomic spacing of each triplet and the angle between them, and it is of the form

TABLE I. Two-body potential parameters.

ij pair		Parameter			
i	*j*	A_{ij}^{rep} (fJ)	ξ_{ij} (Å)	ξ_{ij}^{r} (Å)	C_{ij}^{6} (fJ Å^6)
O	H	0.2283	24	$f(T,P)$[a]	
O	O	0.0425	24	0.610	0.004 226
H	H	0.0000	24	0.000	
Si	O	0.2670	24	0.373	0.007 000
Si	Si	0.0700	24	0.640	
Si	H	0.5000	24	0.350	0.003 800

[a]The ξ_{OH}^{r} parameter is calculated as an empirical function of temperature and pressure as described elsewhere (Ref. 41). The work in this study was all performed at 298 K and 1 atm, and as such, ξ_{OH}^{r} remained constant and took the value of 0.200 010 Å.

$$U_{jik}^{\text{3-body}}(r_{ij},r_{jk},\theta_{jik}) = \lambda_{jik}\exp\left(\frac{\gamma_{ij}}{r_{ij}-r_{ij}^{0}}+\frac{\gamma_{ik}}{r_{ik}-r_{ik}^{0}}\right)\times(\cos\theta_{jik}-\cos\theta_{jik}^{0})^{2}. \quad (8)$$

The effect of this three-body contribution is to bias certain *j-i-k* atomic triplets toward certain angles to emulate the effects of bond directionality without preventing overcoordination, bond angle variations, or imposing any explicit rigidity as is often found in other common interatomic potentials for water. The parameters used are listed in Table III.

B. System assemblage

The vitreous silica portion of the simulated system was created by generating a $64\times64\times42$ Å^3 crystal of stoichiometric β-cristobalite with a total of 11 664 atoms and melting it at 6000 K. The system was simulated at this temperature for 30 000 iterations with a time step of 1 fs for a total of 30 ps to fully randomize the melt and eliminate any residual long-range order. Following this, the system was simulated for 100 000 steps at 4000 K, 100 000 steps at 3000 K, 100 000 steps at 2000 K, 40 000 steps at 1000 K, and 60 000 steps at 298 K with the same time step. The first third of each simulated temperature was carried out in the canonical ensemble to allow equilibration to the temperature, and the remainder was carried out in the microcanonical ensemble. Although volume was constrained during each step of the quench, the system size was rescaled based upon the thermal expansion coefficient of silica at the beginning of each new temperature.

The resulting silica was cleaved in the *x-y* plane by shifting the positions of all atoms occupying the top half of the simulation cell in the +*z* direction, resulting in two unrelaxed silica surfaces separated by a vacuum and with periodic boundaries remaining in all directions. 4851 water molecules were then randomly inserted in the empty volume with a minimum intermolecular spacing of 2 Å to prevent any unusually high-energy configurations from being present in the initial water-silica configuration. This starting configuration system was then simulated with a 0.1 fs time step under conditions of modified *NPT* simulations, with a constant temperature of 298 K and a constant pressure of 1 atm in the *z* dimension, while the dimensions parallel to the water-silica interfaces (*x* and *y*) were fixed.

TABLE II. Point and diffuse charges for each atom.

Species	Si	O	H
Point charge q	+1.808e	−0.904e	+0.452e
Diffuse charge q^d	−0.452e	+0.226e	−0.113e

TABLE III. Three-body potential parameters.

jik triplet			Parameter					
j	*i*	*k*	λ_{jik} (fJ)	γ_{ij} (Å)	γ_{ik} (Å)	r_{ij}^{0} (Å)	r_{ik}^{0} (Å)	θ_{jik}^{0}
O	Si	O	0.0150	2.8	2.8	3.0	3.0	109.5
Si	O	Si	0.0010	2.0	2.0	2.8	2.8	109.5
H	O	H	0.0300	1.3	1.3	1.6	1.6	100.0
Si	O	H	0.0050	2.0	1.2	2.8	1.5	109.5

The starting water-silica configuration was allowed to relax for 2 000 000 steps with a 0.1 fs time step for a total of 200 ps. The high-energy as-cleaved silica surface and the low-density, random dispersion of water molecules reacted significantly during this relaxation process, resulting in hydrated silica interfaces and a significant number of dissociated water products. In addition, the portion of the system occupied solely by water molecules collapsed down under the 1 atm pressure to a 3 nm film of liquid water of normal density (except at the water/silica interfaces, consistent with past results[52]). Details of the behavior of such a 3 nm film of water confined between amorphous silica have shown to reproduce the experimentally observed high thermal expansion of nanoconfined water and are discussed elsewhere.[52]

To better model water-silica systems under conditions of more neutral *p*H, this relaxed water-silica system was then "cleaned" by removing all atoms originally associated as water molecules that were not bound to the silica surface. To maintain charge neutrality of the overall water-silica system, additional protons at the silica surface had to be removed, so all protons adsorbed at BO sites were removed, all adsorbed water molecules ($\equiv$Si$-$OH$_2$) were reduced to silanol ($\equiv$Si$-$OH), and the remainder of the positive charge was removed by reverting silanols deepest into the silica subsurface into non-bridging oxygens (NBO) ($\equiv$Si$-$O$_{\mathrm{NBO}}$). O–H distances less than 1.2 Å were used to define the bonded OH pair, although most O–H bond lengths were considerably shorter than this cutoff, as shown below.

The resulting hydrated silica surfaces were again separated and water molecules were again randomly placed in the void to completely replace the number of equivalent water molecules removed during the cleaning process. This system was then allowed to relax under constant temperature and pressure for another 300 ps, and unless otherwise stated, the data presented were collected from the final 250 ps of this system's simulation.

III. RESULTS AND DISCUSSION

Protonated BO sites formed during the simulation, consistent with previously reported quantum results that indi-

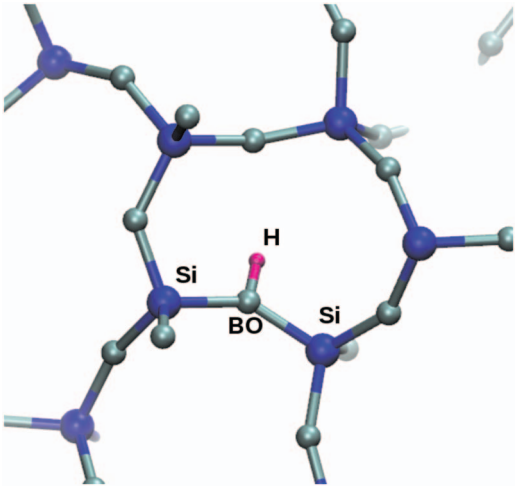

FIG. 1. Representation of a H on a BO. Large blue atoms represent silicon, smaller gray atoms represent oxygen, and small red atom is hydrogen. Si–O bonds are drawn for Si–O separations less than 2.0 Å. Not all atoms and bonds are drawn in the image, so that the apparent NBO are actually BO to Si not drawn.

cated that the formation of these BOH sites is either thermodynamically preferred[45] or has a relatively low activation barrier.[46] Figure 1 depicts such a representative BOH at the water-silica interface. The average concentration of these BOH sites at any given moment during the final 100 ps of the simulation was 0.181 nm^{-2}, which is an order of magnitude smaller than the surface density of silanol (commonly reported to be around 4.6 nm^{-2}) and a very small fraction of the total siloxane bridges exposed at the surface. The following analysis of these BOH sites reflects data sampled at 500 fs intervals during the simulation unless otherwise noted.

BO sites will be divided into two subcategories based on whether or not the bridge was found to be an adsorption site for protons. The bridges which were observed with an adsorbed proton in at least one of the sampled configurations will be referred to as *BOH sites*, and those bridges which never possessed an adsorbed proton throughout the sampled configurations will be referred to as *dry bridging sites*. Similarly, a bridging site with an adsorbed proton at the moment in question will be referred to as a *BOH*, and a bridging site without any adsorbates will be referred to as a *dry bridge*. By these definitions, a dry bridging site is always a dry bridge, but a BOH site may be a BOH or a dry bridge depending on its current state of protonation.

A. Characterization of bridging OH sites

Protons were found to adsorb on only 150 of the 2379 oxygen bridges within 7 Å of the water-silica interfaces, indicating that proton adsorption occurs only under certain circumstances. To determine what factors may predispose certain dry bridges to proton adsorption (thus being labeled BOH sites), several structural parameters were calculated for all of these near-surface siloxane bridges. The size of the smallest ring to which each bridge belonged was calculated, and the angular and linear strain in the silicon-oxygen bonds of each bridge was found. Although both BOH sites and dry bridging sites were examined, the strain in BOH sites was

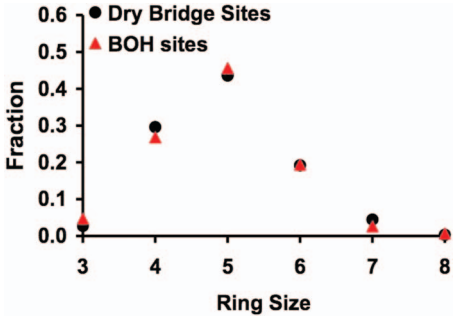

FIG. 2. Ring size distribution of the BO atoms that were observed to be adsorption sites for protons, called bridging OH (BOH), and the distribution of all dry surface siloxane rings.

only averaged over the time that BOH site was dry to exclude any additional strain that may have been caused by the adsorbed proton.

BOH sites were found to form on rings of all sizes with equal probability, as shown in Fig. 2, with the majority of BOH sites occurring on four-, five-, and six-membered rings. However, the angular strain of BOH sites was found to be consistently higher than in dry bridging sites near the surface, with protons preferring siloxane bridges with more acute angles, as shown in Fig. 3. The average angle of a BOH site in the absence of an adsorbed proton was 142.7°; by comparison, the average angle of dry siloxane bridges was found to be 150.2°. Thus, those siloxane bridges which eventually attract a hydrogen ion have an average bond angle significantly less than the average angle of dry bridging sites.

It should be emphasized that the angles reflected in Fig. 3 weight each BOH site equally rather than by the stability of the proton at a site. Because most of the BOH sites that were examined supported an adsorbed proton for only a brief duration, the average angles presented in Fig. 3 are biased toward the angles of those bridges which support transient proton adsorbates. Thus, these angles do not represent the lowest energy, most ideal bridging angle for protonated bridges; rather, they illustrate that those bridges that can attract protons have smaller siloxane bond angles than those bridges that cannot. This is in agreement with the *ab initio*

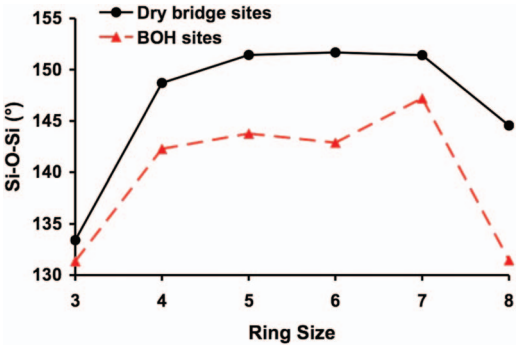

FIG. 3. Average bridging angle as a function of ring size for BOH sites and bridges that do not become protonated. For reference, the mean bridging angle in vitreous silica is in the vicinity of 150°, consistent with the average angle of dry bridge sites. Note that the average angles for BOH sites weigh all sites equally. As a result, the angle of a site which sustained a proton for a long period of time contributed to the average angle with the same weight as a site which sustained a proton very briefly.

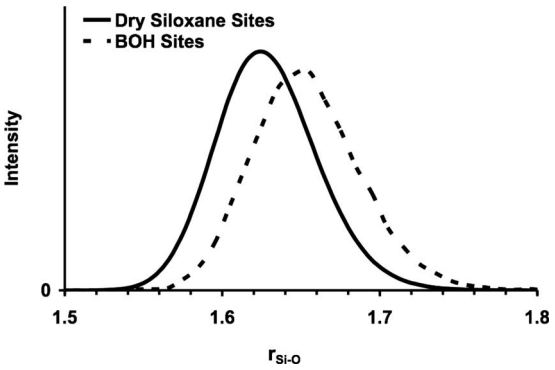

FIG. 4. First peak in the normalized Si–O pair correlation function. Dashed line corresponds to the pair correlation function around oxygen coordinated to two silicons and one hydrogen (BOH); solid line corresponds to the pair correlation function around oxygen coordinated to only two silicons (siloxane bridges).

calculation by Geisinger *et al.*[35] that showed the BOH has a 10.5° lower bond angle than the dry bridge. Most importantly, the MD simulation results in Fig. 3 indicate that all of the different ring sizes possess these smaller angle bridging sites that can act as adsorption sites for the proton. The relation between bond angles and proton stability is presented in more detail below in the discussion of BOH lifetimes.

The pair correlation function between BOs and their silicon neighbors was calculated and the first Si–O peaks for both dry siloxane sites and BOH sites are shown in Fig. 4. Sites that are conducive to proton adsorption have strained Si–O bonds with an average elongation of between 0.02 and 0.03 Å and an average bond centered at 1.650 Å. While this elongated bond is significantly smaller than the 1.709–1.821 Å final bond lengths predicted by quantum cluster models,[35,45,46] like Fig. 3, these data are averaged over all BOH sites, even those that form a very transient BOH, meaning that the bond lengths are not representative of the most stable BOH sites. It is also likely that bonds greater than 1.7 Å would have reacted with water and ruptured early during the relaxation simulation; thus, the BOH site peak in Fig. 4 represents those sites which are conducive to proton adsorption but resist rapid H^+-catalyzed bond rupture and dissolution reactions.[45]

B. Response of siloxane to protonation

Although *ab initio* calculations of $H_7Si_2O_7^+$ dimers suggest that the adsorption of a proton to a bridge is associated with narrower bridging angles and longer Si–O bonds, it is not clear whether the bond strain is the effect of proton adsorption or the cause of it. For example, quantum calculations by Pelmenschikov *et al.*[11] showed a significant difference in the susceptibility of a Si–O bond to hydrolysis between a free molecular cluster and a cluster that is restricted in relaxation to account for the effects of solid connectivity. This indicates that the angular response of isolated $H_7Si_2O_7^+$ molecules to proton adsorption may not accurately represent the response of a siloxane bridge embedded in an amorphous surface. Thus, for the sake of determining whether protonation is biased toward prestrained siloxanes or if protonation causes strain, the behavior of individual BOH sites in both the protonated and dry states was examined.

This comparison of BOH sites while protonated and dry reveals that the bridging angle of these sites shows a statistically negligible decrease upon protonation. 75% of BOH sites showed a smaller average bridging angle when protonated than when deprotonated, while 21% were found to have a wider average angle, and the final 4% remained protonated throughout the course of the final 100 ps of simulation. However, the average decrease in angle was found to be 2.2°, while the standard deviation in any given BOH site's angle averaged 3.3° at 298 K. Thus, if there is a true tendency for the bridging angle to decrease upon proton adsorption, the change is slight, indicating the importance of using a sufficiently large silica surface to include the effects of network connectivity (consistent with the conclusions by Pelmenshikov *et al.*[11]) and the heterogeneity in ring structures in the surface.

The Si–O bonding distance for all BOH was found to follow similar behavior. 78% of BOH sites show an elongation of the Si–O bond while protonated and 17% show a decrease. The average decrease of 0.015 Å is commensurate to the standard deviation in any given Si–O bond's measure of 0.018 Å though, so the effect of protonation on the Si–O bond length is also very slight and wholly within the thermal vibration amplitude at room temperature. Based on this, the overall effect of proton adsorption on a siloxane bridge is minimal in the constrained bonding environment of a silica surface.

Thus, the formation of BOH at the silica surface is a consequence of pre-existing strained sites, and the presence of a proton near an otherwise low-energy bridge will not cause that site to undergo the deformation necessary to make proton adsorption favorable. This is in qualitative agreement with the conclusions put forth by Criscenti *et al.*[46] that proton adsorption onto a stable bridge is not energetically favorable, and this resistance to deformation on protonation coincides with the *ab initio* calculations of Pelmenschikov *et al.*[11] previously mentioned. However, due to the distribution of bridging angles inherent in vitreous silica surfaces, there will exist a concentration of bridges that are sufficiently strained to enable proton adsorption without the rapid H^+ catalyzed hydrolysis proposed by Xiao and Lasaga.[45]

C. Conditions for proton adsorption

Because the geometry of a BOH site changes only marginally as a consequence of protonation, the overall concentration of BOH will vary with the concentration of strained siloxanes at the surface and the magnitude of their strain. To determine the stability of BOH on bridges of differing strain, the average O–H bond length for each BOH that occurred throughout the final 100 ps of the simulation was classified according to its simultaneous bridging angle. The range of encountered bridging angles was divided into increments of 2° and the O–H distance of all BOH groups in each increment was averaged. The result of this calculation is shown in Fig. 5, which quantitatively shows that bridges with smaller bond angles allow the adsorbed proton to be physically

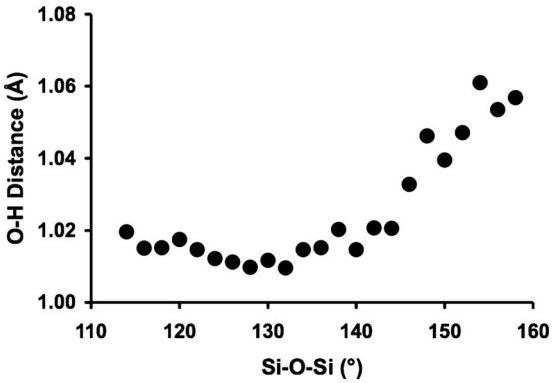

FIG. 5. Average O–H separation distance as a function of bridging angle for BOH groups. O–H distances were averaged over intervals of 2°. Data for bridges with an angle greater than 160° are not shown; these high-angle data comprised only 0.6% of the total measurements and were prone to very high scatter as a result.

closer to the oxygen. This translates to a stronger bond between oxygen and hydrogen and, most likely, a greater stability of the proton on the bridge, a decreased likelihood of deprotonation or proton transport, and an increased likelihood of H^+-catalyzed hydrolysis.

To determine which angles are most energetically favorable, the potential energy of the oxygen atom central to each BOH in the final 100 ps of the simulation was also explicitly calculated for the duration of its protonation. The energy of the BO in all dry siloxane sites near the surface was also calculated and averaged in intervals of 0.5° over the entire range of angles observed. The results are shown in Fig. 6, revealing that there is a definite minimum energy angle for a protonated bridge that lies between 125° and 135°, while dry siloxane bridges have approximately the same energetic preference for a much wider range of angles. These findings coincide almost exactly with the results obtained from first-principles calculations by Geisinger *et al.* [see their Fig. 4(a) (Ref. 35)] and Vanheusden *et al.* [see their Fig. 6 (Ref. 50)], giving a strong indication that a concentration of these BOH sites will form at bridges whose angles are between 125° and 135°. This is corroborated by the data shown in Fig. 7 which

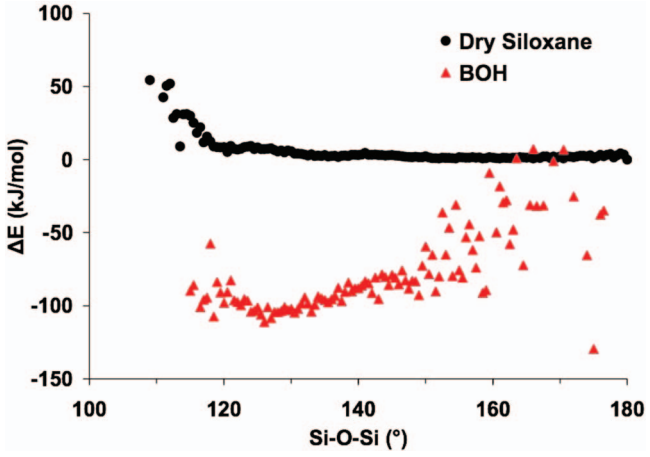

FIG. 6. Energy of BOs as a function of bridging angle. Energies are referenced to the energy of widest dry siloxane bridge encountered for ease of comparison. The data were averaged in 0.5° intervals, and scatter at the extremes is due to small available sample sizes.

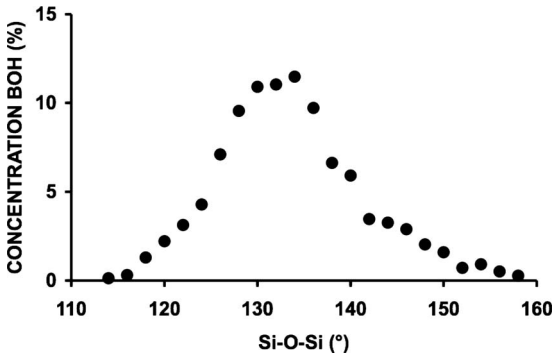

FIG. 7. Concentration of BOH (%) as a function of Si–O–Si bond angle, showing the significant distribution of BOH in the ~130°–135° range, consistent with *ab initio* calculations and Figs. 4 and 5.

show the number of BOH that contributed to the data in Figs. 5 and 6, indicating that BOH in the low 130°'s range make the largest concentration of sites. Again, these findings from MD simulations are consistent with previous *ab initio* calculations yet sample a heterogeneous silica surface rather than specific predetermined sites.

The variation in energy with bond angle for BOH groups in Fig. 6 also shows the same features as the variation in O–H separation in Fig. 5, indicating that the energy change due to protonation is most closely related to the O–H separation distance on the BOH and not the change in angular or linear bond strain in the bridge. Since this O–H distance varies with the bridging angle as shown in Fig. 5, this is a further indication that the stability of BOH sites and their ability to form is governed primarily by the angle of the dry bridge precursor, and the effects of the Si–O distance and any relaxation that may occur after protonation are minor by comparison. This rigidity is an effect of the network connectivity, as considered by Pelmenschikov *et al.*,[11] and further stresses the significance of simulating extended silica surfaces rather than flexible molecular analogs.

D. Stability of bridging OH

To determine the lifetimes of protonated bridges more accurately, the changes in the coordination of all oxygen species in the system were tracked throughout the final 100 ps of the simulation every femtosecond. The lifetime of protons adsorbed to bridging sites was determined by examining those sites which entered the final 100 ps of the simulation as dry bridges, became protonated, then deprotonated, and finished the simulation as a dry bridge again. As mentioned above, an O–H distance of less than 1.2 Å was used to define protonation of a site. Those bridges which entered the final 100 ps of simulation already protonated or became protonated but never deprotonated by the conclusion of the simulation were discounted because the full length of the dry to protonated to dry state could not be ascertained.

During this final 100 ps, those BOH that formed were found to have predominantly very short lifetimes of under 20 fs. The number of longer-lived protonated bridges drops off sharply for lifetimes above 20 fs, indicating that proton behavior on strained bridges is very dynamic with rapid adsorption and desorption. Kurtz and Karna[49] calculated a very

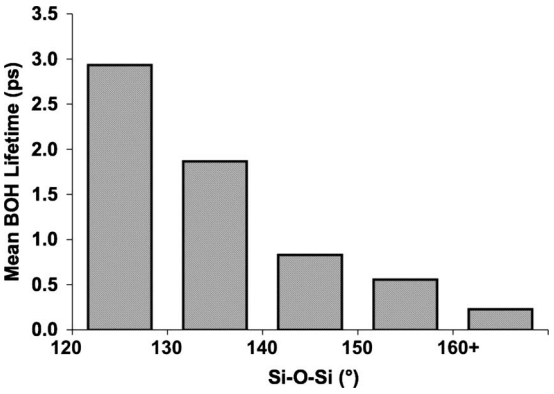

FIG. 8. Adsorbed proton lifetime as a function of the bridging angle on the adsorbing site. Note that because BOH sites tend to exhibit several long adsorption lifetimes amidst a number of very quick adsorption/desorption reactions, the mean lifetimes in this diagram include only the lifetimes measured for BOH which remained protonated for more than 0.1 ps.

low activation energy barrier to proton transport across ideally located BOs in a siloxane ring (0.1–0.2 eV), recognizing that further transfers would require significant flexibility in the ring. Such flexibility is minimal due to the connectivity of the rings in the network. The presence of adjacent water molecules provides the additional path for proton transport to other surface sites, as seen in the current simulations. Bridges with sufficient strain to negate the energetic barrier but not hydrolyze the bridge will still not stably bind protons. As a consequence, the strained bridges at the silica surface predominantly serve as temporary repositories for excess protons, in contrast to the more permanent silanol groups.

While the majority of observed BOH remained protonated for less than 100 fs, it should be noted that these data implicitly presume that all BOH formations are unrelated. Examination of individual BOH sites, though, revealed that 63% of the 276 BOH sites contributed more than one lifetime because of multiple instances of protonation followed by deprotonation. Furthermore, 20% of the 276 sites were observed to undergo protonation in excess of five times, and the difference in lifetime for these sites which underwent multiple protonations varied, in many cases, by an order of magnitude or more. This indicates that the process of proton adsorption on a BO involves spatial oscillations of the proton prior to or following the adsorption event that produces the long-lived BOH. This is consistent with the behavior of proton transport in water, where the proton can oscillate between the oxygens of the reacting molecules in the Zundel complex prior to the final transfer.[15,41,47,53]

In light of this observation, those adsorbed protons that had lifetimes of less than 0.1 ps were discounted as being transient proton oscillations for the purposes of calculating the average lifetime of BOH. As a result of this discretion, only 28% of the individual lifetimes measured were considered to be significant, and only 52% of the 276 BOH sites were found to support adsorbed protons for longer than 0.1 ps. Of these BOH sites that remained stable for more than 0.1 ps though, the average lifetime was found to be around 1.2 ps; however, the true lifetime was found to depend greatly on the bridging angle. Figure 8 shows this and, as would be inferred by the other trends presented, siloxane bridges with a greater degree of angular strain result in protons, which remain adsorbed for significantly longer.

It should be emphasized again that these data only reflect the adsorption lifetimes of protons for which both the adsorption and desorption were observed within the final 100 ps of simulation; not included are a total of 22 BOH whose lifetimes could not be determined exactly. Five BOH groups persisted stably throughout the final 100 ps, and consistent with the measurable lifetimes discussed above, the average bridging angle of these stable BOH groups was 131°. Ten more bridges began the final 100 ps of simulation with an adsorbed proton, and seven bridges became protonated during the final 100 ps and remained that way through the end of the simulation. Of these 17 protonated bridges, those whose minimum possible lifetimes exceeded 1 ps had an average lifetime not less than 45.9 ps and an average bridging angle of 134°. These lifetimes are far in excess of the values shown in Fig. 8 and indicate that protons have the ability to remain adsorbed to narrow bridges for long periods of time without undergoing deprotonation or hydrolysis of the bridge. Of course, the binding energy of these protons is significantly less than that of a proton at a hydroxyl site, providing a highly acidic site on the silica surface that may be relevant to the bimodal pK, of silica.

The implications of these metastable BOH sites at the silica surface are potentially far reaching. Enhanced proton conduction in silica-based glasses has been observed in the presence of water,[30] and the current atomistic model for this behavior regards molecular water as the enabling species which allows hydronium formation and accelerated proton transfer in the liquid near the surface.[15,30,37] However, the presence of strained siloxanes that are acidic surface groups serve as ideal intermediate steps in proton transfer near the surface.

It is therefore probable that in addition to hydronium formation and water-assisted proton transfer in the liquid, protons can rapidly move across the water-silica interface via strained bridges that are predisposed to transient proton adsorption. Thus, an excess proton at any given location on a silica surface can move by either water-assisted or strained bridge-assisted diffusion depending on the local environment. The result of this would be net migration that is faster than it would be if only one mechanism is possible.

IV. CONCLUSIONS

MD simulations indicate that the protonation of BO at the surface of vitreous silica occurs at sites with a bridging angle well below the bulk silica mean of ~150°. The simulations also show that the distribution of angular strain present in vitreous silica allows a number of sites to be predisposed to proton adsorption. The bridges most likely to be adsorption sites have a bridging angle between 125° and 135°, and the energy differences between dry and protonated bridges at various angles observed in the simulations coincide completely with quantum calculations over the entire range of bridging angles encountered in the vitreous silica surface. Those sites with bridging angles near 130° also support adsorbed protons more stably, resulting in the proton

remaining adsorbed for longer periods of time. However, the process of proton adsorption and desorption was found to be very dynamic, with stable adsorption being preceded or followed by very short-lived oscillations.

The effect of the linear strain in the Si–O bond has much less of an effect on making a site conducive to protonation in contrast to first-principles calculations based on molecular analogs, and this is due to the lack of flexibility of neighboring SiO_4 tetrahedra when embedded in a solid surface in contrast to molecules which are unconstrained at three of each of the tetrahedron's four vertices. Another result of this structural rigidity is the relatively minor geometric response to proton adsorption; the change in linear and angular strain before and after proton adsorption is very slight. Thus, BOH sites are less likely to form on crystalline surfaces which have a very narrow distribution of bridging angles, but vitreous silica has the necessary distribution of angular strain over all ring sizes to allow protons to adsorb to bridges at the surface.

These simulation results indicate the importance of performing large size and time scale simulations of the structurally heterogeneous vitreous silica exposed to water to describe proton transport at the interface between water and the silica surface.

ACKNOWLEDGMENTS

G.K.L. acknowledges support from the Advanced Fuel Cycle Initative University Fellowship sponsored by the DOE Office of Nuclear Energy.

[1] R. K. Iler, *The Colloid Chemistry of Silica and Silicates* (Cornell University Press, Ithaca, 1955).
[2] R. K. Iler, *The Chemistry of Silica* (Wiley, New York, 1979).
[3] B. A. Morrow, I. A. Cody, and L. S. M. Lee, J. Chem. Phys. **80**, 2761 (1976).
[4] B. Bunker, D. Haaland, T. Michalske, and W. Smith, Surf. Sci. **222**, 95 (1989).
[5] B. C. Bunker, D. M. Haaland, K. J. Ward, T. A. Michalske, W. L. Smith, and C. A. Balfe, Surf. Sci. **210**, 406 (1989).
[6] C. J. Brinker, R. K. Brow, D. R. Tallant, and R. J. Kirkpatrick, J. Non-Cryst. Solids **120**, 26 (1990).
[7] L. T. Zhuravlev, Langmuir **3**, 316 (1987).
[8] I.-S. Chuang and G. E. Maciel, J. Am. Chem. Soc. **118**, 401 (1996).
[9] B. P. Feuston and S. H. Garofalini, J. Appl. Phys. **68**, 4830 (1990).
[10] A. G. Pelmenschikov, G. Morosi, and A. Gamba, J. Phys. Chem. **96**, 7422 (1992).
[11] A. Pelmenschikov, H. Strandh, L. G. M. Pettersson, and J. Leszczynski, J. Phys. Chem. B **104**, 5779 (2000).
[12] A. A. Hassanali and S. J. Singer, J. Phys. Chem. B **111**, 11181 (2007).
[13] N. Sahai, Environ. Sci. Technol. **36**, 445 (2002).
[14] J. R. Rustad, E. Wasserman, A. R. Felmy, and C. Wilke, J. Colloid Interface Sci. **198**, 119 (1998).
[15] T. S. Mahadevan and S. H. Garofalini, J. Phys. Chem. C **112**, 1507 (2008).
[16] S. Hamad and S. T. Bromley, Chem. Commun. (Cambridge) **2008**, 4156.
[17] R. Wang and S. L. Wunder, Langmuir **16**, 5008 (2000).
[18] V. Kocherbitov and V. Alfredsson, J. Phys. Chem. C **111**, 12906 (2007).
[19] D. A. Sverjensky and N. Sahai, Geochim. Cosmochim. Acta **62**, 3703 (1998).
[20] J. A. Tossell and N. Sahai, Geochim. Cosmochim. Acta **64**, 4097 (2000).
[21] M. C. F. Wander and A. E. Clark, J. Phys. Chem. C **112**, 19986 (2008).
[22] T. Bakos, S. N. Rashkeev, and S. T. Pantelides, Phys. Rev. B **69**, 195206 (2004).
[23] W. A. Adeagbo, N. L. Doltsinis, K. Klevakina, and J. Renner, ChemPhysChem **9**, 994 (2008).
[24] M. J. Matthewson and C. R. Kurkjian, J. Am. Ceram. Soc. **71**, 177 (1988).
[25] Q.-Y. Tong and U. Gosele, *Semiconductor Wafer Bonding: Science and Technology* (Wiley, New York, 1999).
[26] G. V. Gibbs, Am. Mineral. **67**, 421 (1982).
[27] A. C. Lasaga and G. V. Gibbs, Phys. Chem. Miner. **14**, 107 (1987).
[28] M. D. Newton and G. V. Gibbs, Phys. Chem. Miner. **6**, 221 (1980).
[29] K. Ferrand, A. Abdelouas, and B. Grambow, J. Nucl. Mater. **355**, 54 (2006).
[30] M. Nogami and Y. Abe, Phys. Rev. B **55**, 12108 (1997).
[31] M. Nogami, R. Nagao, and C. Wong, J. Phys. Chem. **102**, 5772 (1998).
[32] M. Nogami, J. Sol-Gel Sci. Technol. **31**, 359 (2004).
[33] M. O'Keeffe and G. Gibbs, J. Chem. Phys. **81**, 876 (1984).
[34] B. C. Chakoumakos and G. V. Gibbs, J. Phys. Chem. **90**, 996 (1986).
[35] K. L. Geisinger, G. V. Gibbs, and A. Navrotsky, Phys. Chem. Miner. **11**, 266 (1985).
[36] A. C. Lasaga and G. V. Gibbs, Am. J. Sci. **290**, 263 (1990).
[37] Y. Ma, A. S. Foster, and R. M. Nieminen, J. Chem. Phys. **122**, 144709 (2005).
[38] T. R. Walsh, M. Wilson, and A. P. Sutton, J. Chem. Phys. **113**, 9191 (2000).
[39] S. H. Garofalini, J. Non-Cryst. Solids **120**, 1 (1990).
[40] B. F. Feuston and S. H. Garofalini, J. Phys. Chem. **94**, 5351 (1990).
[41] T. S. Mahadevan and S. H. Garofalini, J. Phys. Chem. B **111**, 8919 (2007).
[42] P. Gallo, M. A. Ricci, and M. Rovere, J. Chem. Phys. **116**, 342 (2002).
[43] Z. M. Du and N. H. de Leeuw, Dalton Trans. **22**, 2623 (2006).
[44] Y. Duval, J. A. Mielczarski, O. S. Pokrovsky, E. Mielczarske, and J. J. Ehrhardt, J. Phys. Chem. B **106**, 2937 (2002).
[45] Y. Xiao and A. C. Lasaga, Geochim. Cosmochim. Acta **58**, 5379 (1994).
[46] L. J. Criscenti, J. D. Kubicki, and S. L. Brantley, J. Phys. Chem. A **110**, 198 (2006).
[47] M. Tuckerman, K. Laasonen, M. Sprik, and M. Parrinello, J. Phys. Chem. **99**, 5749 (1995).
[48] K. Vanheusden, W. L. Warren, R. A. B. Devine, D. M. Fleetwood, J. R. Schwank, M. R. Shaneyfelt, P. S. Winokur, and Z. J. Lemnios, Nature (London) **386**, 587 (1997).
[49] H. A. Kurtz and S. P. Karna, IEEE Trans. Nucl. Sci. **46**, 1574 (1999).
[50] K. Vanheusden, P. P. Korambath, H. A. Kurtz, S. P. Karna, D. M. Fleetwood, W. M. Shedd, and R. D. Pugh, IEEE Trans. Nucl. Sci. **46**, 1562 (1999).
[51] D. Wolf, P. Keblinski, S. R. Phillpot, and J. Eggebrecht, J. Chem. Phys. **110**, 8254 (1999).
[52] S. H. Garofalini, T. S. Mahadevan, S. Xu, and G. W. Scherer, ChemPhysChem **9**, 1997 (2008).
[53] D. Marx, M. E. Tuckerman, and M. Parrinello, J. Phys. Condens. Matter **12**, A153 (2000).